Indistinguishable Entangled Photons Generated by a Light-Emitting Diode

R. M. Stevenson,[1] C. L. Salter,[1,2] J. Nilsson,[1] A. J. Bennett,[1] M. B. Ward,[1] I. Farrer,[2] D. A. Ritchie,[2] and A. J. Shields[1]

[1]*Toshiba Research Europe Limited, 208 Science Park, Cambridge CB4 0GZ, United Kingdom*

[2]*Cavendish Laboratory, University of Cambridge, JJ Thomson Avenue, Cambridge CB3 0HE, United Kingdom*

(Received 3 August 2011; published 27 January 2012)

A linear optical quantum computer relies on interference between photonic qubits for logic, and entanglement for near-deterministic operation. Here we measure the interference and entanglement properties of photons emitted by a quantum dot embedded within a light-emitting diode. We show that pairs of simultaneously generated photons are entangled, and indistinguishable from subsequently generated photons. We measure entanglement fidelity of 0.87 and two-photon-interference visibility of 0.60 ± 0.05. The visibility, limited by detector jitter, could be improved by optical cavity designs.

DOI: 10.1103/PhysRevLett.108.040503 PACS numbers: 03.67.Bg, 03.65.Ud, 42.50.Dv, 78.67.Hc

One promising design of a scalable quantum computer encodes qubits using single photons, and employs optical components such as beam splitters with photodetection, to enable interactions between photons and implement probabilistic quantum gates [1]. Many qubits and gate operations are required in order to process a quantum algorithm that will offer an advantage over conventional digital logic, which makes the use of probabilistic gates impractical. However, by using additional entangled photons the gate success probability can be increased arbitrarily close to one using the feed-forward technique [1].

In addition to entanglement between photons, interactions between photonic qubits rely on two-photon interference, and thus the individual photonic qubits must be indistinguishable. By linking multiple pairs of entangled photons this way, larger multipartite entangled states may be created [2,3]. Parametric down-conversion sources of entangled light have been shown to produce indistinguishable photons [4], typically aided by spectral filtering of the output beams, and have been employed in small scale quantum logic experiments [5–9]. However, the probabilistic nature of the down-conversion process often generates zero or multiple photon pairs following a Poissonian distribution, which leads to errors in quantum algorithms [10] and renders such sources unsuited to deterministic quantum computing.

In contrast, semiconductor quantum dots fundamentally generate non-Poissonian, quantum states of light such as single photons [11] and entangled photon pairs [12]. Interaction between indistinguishable single photons has been reported [13], but not indistinguishability of entangled photons. Crucially, entangled light emission from quantum dots can now be controlled and generated electrically [14,15], something not yet possible for other non-Poissonian quantum light sources such as those based on atomic transitions. This potentially allows integration of many devices onto single, voltage-operated chips, which is expected to be of great practical advantage when realizing large quantum logic circuits.

However, until now, correlations and interactions between photons from non-Poissonian light sources have only been observed for photon pairs. Here we generate up to four photons from two radiative decay cycles of a quantum dot. We show that photons emitted with different energy during the same decay process are entangled, and additionally photons emitted with the same energy from different decay cycles can interact and are indistinguishable. Such interactions can facilitate entanglement of two photons originating from independent pairs through entanglement swapping [16], which is an important quantum operation used in quantum repeaters [17] and for entanglement purification [18].

The quantum dot entangled light source investigated here is based on a single nominally InAs quantum dot embedded within the GaAs intrinsic region of a resonant cavity LED operating at ~5 K [15]. Entangled photon pairs may be generated by the radiative decay of the biexciton state to the ground state [19]. For quantum dots emitting close to 1.4 eV, the fine-structure splitting (FSS) between the intermediate exciton spin states is minimized [20]. This leads to the emission of polarization-entangled exciton-biexciton photon pairs of high fidelity with the entangled Bell state $|\Psi^+\rangle = (|H_{XX}H_X\rangle + |V_{XX}V_X\rangle)/\sqrt{2}$ where H, V, X, and XX represent horizontally and vertically polarized photons of the exciton and biexciton states, respectively.

Light emitted by the quantum dot was collected by a microscope objective lens and coupled to polarization maintaining (PM) single mode fiber. The emission spectrum was measured by a spectrometer and CCD and is shown in Fig. 1(a), for a typical dc driving current of 70 nA μm^{-2}. The spectrum is dominated by the neutral X and XX emission lines due to the heterostructure design [15]. Other weak lines observed in this region of the spectrum are probably charged exciton emission lines associated with the same quantum dot. In contrast, charged exciton emission lines dominate in previous reports of interference of electrically generated single photons

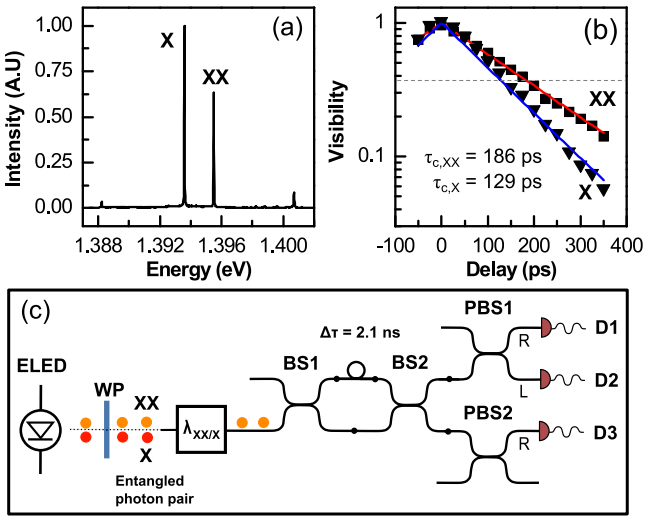

FIG. 1 (color online). (a) Spectrum of emission from the entangled-light-emitting diode. (b) Visibility of exciton (X) and biexciton (XX) single-photon interference as a function of the time delay in a Michelson interferometer. The solid lines are fitted exponential decay. Dotted line is $1/e$. (c) Schematic of the fiber-based two-photon interferometer. Components include an entangled-light-emitting diode (ELED), wave plate (WP), monochromator set at wavelength λ_X or λ_{XX}, beam splitters (BS1 and BS2), polarizing beam splitters (PBS1 and PBS2), and photon detectors (D1–D3).

[21,22]. The fine-structure splitting between the exciton spin eigenstates was measured to be 2.0 ± 0.2 μeV.

The coherence properties of the individual photons emitted by the device are critical to indistinguishability and the success of a two-photon interference experiment. Using a free-space Michelson interferometer we have measured coherence times τ_c of X and XX photons generated by many different quantum dots that emit around 1.4 eV. Typical values are a few 100 s of picoseconds, comparable to optically excited devices [23]. A suitable quantum dot was selected for further study that has considerably improved τ_c compared to a previously reported device from an earlier wafer [15]. Under typical dc injection conditions the visibility of single-photon interference decays approximately exponentially with the interferometer time delay, characterized by a coherence time τ_c of 186 ps for XX photons, and 129 ps for X photons, as shown in Fig. 1(b). τ_c is found to decrease with increasing injection current, indicative of homogeneous broadening [21].

Polarization-dependent second-order correlation measurements were used to determine the entanglement and two-photon-interference (TPI) properties of emitted photon pairs. Selection of the polarization measurement basis was achieved by an appropriately oriented half- or quarter-wave plate inserted directly after the microscope lens. Fiber coupled monochromators were used to spectrally isolate X and XX emission without reducing linewidth. Polarizing fiber beam splitters were used to analyze the polarization of photons before detection using commercial superconducting single photon detectors (SSPDs). The time delay between photon detection events τ was recorded with time resolution of $\sim$140 ps. We use the notation $g_M^{(2)}(P_1P_2, \tau)$ to represent the normalized second-order correlation function, where M denotes the TPI or entanglement (E) measurements, P_1 and P_2 denote the polarizations measured in each of the two-photon-channels.

The entanglement properties between the emitted X-XX photon pairs were determined from co- and crosspolarized second-order correlation measurements in the rectilinear, diagonal, and circular polarization basis, as shown in Figs. 2(a)–2(c). For small negative delays, $g_E^{(2)}$ reduces to

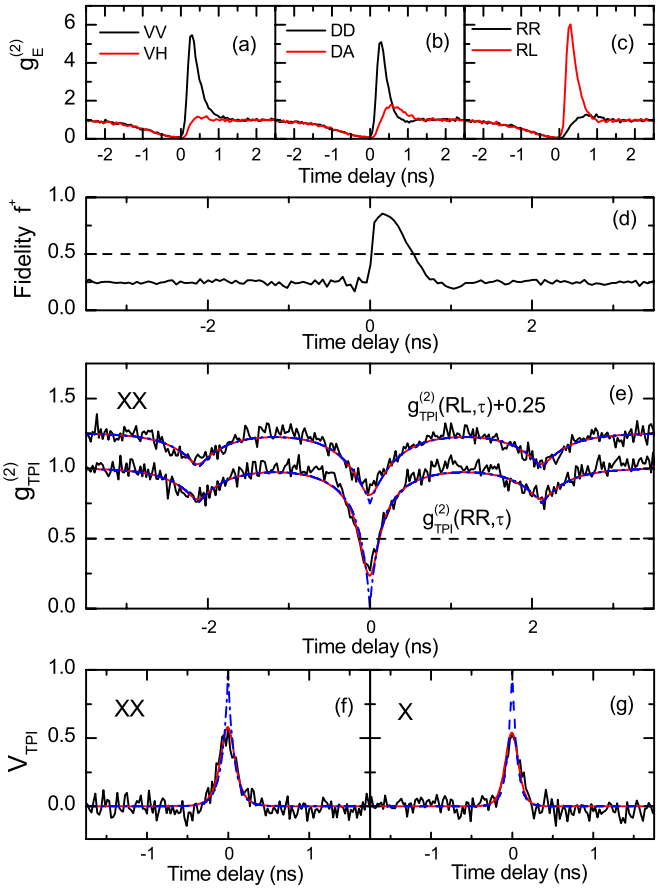

FIG. 2 (color online). Second-order correlation of photon pairs emitted by the entangled LED in dc mode, measured in the (a) rectilinear, (b) diagonal, and (c) circular polarization bases. Co- and crosspolarized measurements are represented by black and gray (red online) lines, respectively. (d) Fidelity f^+ of the emission to the entangled Bell state $|\Psi^+\rangle$. The classical limit of 0.5 is represented by a dashed line. (e) Second-order correlation of pairs of XX photons exiting the two-photon interferometer. The crosspolarized correlation $g_{\mathrm{TPI}}^{(2)}(\mathrm{RL}, \tau)$ is vertically displaced by 0.25 so it may be distinguished from the copolarized correlation $g_{\mathrm{TPI}}^{(2)}(RR, \tau)$. (f) and (g) Visibiltiy of XX and X TPI. Solid and dashed curves in (e),(f), and (g) are simulated behavior for actual and ideal detector performance, respectively.

an average minimum value of 5.9%, which is very low compared to similar entanglement measurements on another quantum dot within an LED [15] where the value was ~30%, and approximates ideal behavior of $g_E^{(2)}(0) = 0$ more closely. This is attributed to the higher temporal resolution of the SSPDs and improved background light rejection due to the spatial filtering effect of coupling to single mode fiber compared to the avalanche photodiode detectors and free-space collection system used in previous experiments. For small positive delays, strong polarization correlations are observed in the copolarized linear bases and the crosspolarized circular basis. This is the expected behavior of the Bell state $|\Psi^+\rangle$.

The fidelity of the emitted photon pairs with $|\Psi^+\rangle$ was determined from the above $g_E^{(2)}$ measurements [23], and is plotted in Fig. 2(d). The maximum achieved fidelity is 0.85 ± 0.01, which is the highest value reported to date for an electrically driven entangled light source.

Two-photon interference was measured using a PM fiber based interferometer, as shown in Fig. 1(c). Interference between subsequent X or XX photons was measured independently, by selecting photons at the wavelength of interest with a monochromator. The filtered emission was divided into two arms with a 50/50 coupler BS1. Photons in one arm were delayed by an additional 2.1 ns, much longer than τ_c, before recombining at a 50/50 coupler BS2. The time delay between pairs of subsequent photons was postselected by temporal measurement [21], in contrast to some two-photon-interference experiments which employ variable delay lines to control the delay between incident photons [4]. Additionally, and in contrast to previous two-photon interference experiments with quantum dots [13,24,25], the unpolarized nature of the entangled photon pair emission process means that the polarization of the X or XX photon pairs may also be postselected. Thus interfering and noninterfering photon pairs can be measured in the same experiment. This is achieved using fiber polarization splitters PBS1 and PBS2 on each output from BS2, and recording co- and crosspolarized coincidences.

The measured co- and crosspolarized second-order correlations $g_{\mathrm{TPI}}^{(2)}$ are shown in Fig. 2(e) for pairs of XX photons. The dips at ± 2.1 ns are attributed solely to the sub-Poissonian nature of the source, as there is no contribution from two XX photons entering the long and short arm of the interferometer simultaneously. For the crosspolarized trace, $g_{\mathrm{TPI}}^{(2)}(\mathrm{RL}, \tau)$ dips to approximately 0.5 at zero delay. This is also due to the sub-Poissonian nature of the source, as there is no contribution from two XX photons entering the same arm of the interferometer simultaneously. For copolarized photon pairs, the dip at zero delay is significantly deeper than observed for crosspolarized photons. This reduction in coincidence intensity indicates that copolarized XX photon pairs are preferentially exiting the same port of coupler BS2. This is a clear indication of two-photon interference; when two indistinguishable photons are incident on opposite ports of BS2, destructive interference of the joint-detection amplitude of the photon pair state means the photon detection in opposite ports of BS2 is suppressed [4].

The visibility of the interference is commonly used to quantify the extent to which the photons have interacted, and is defined as $(g_\perp^{(2)} - g_\parallel^{(2)})/g_\perp^{(2)}$, where $g_\parallel^{(2)}$ and $g_\perp^{(2)}$ are the co- and crosspolarized second-order correlations, respectively, and is plotted in Fig. 2(f) for pairs of XX photons. For delays between photons greater than a few hundred picoseconds, the visibility is close to zero, consistent with the measured coherence time of the XX photons. However, for photons detected at similar times, the visibility is nonzero, indicating that two-photon interference has taken place. Similar results are observed for pairs of X photons as shown in Fig. 2(g), though the width of the visibility peak is narrower due to the shorter coherence time. However, the detrimental effect of shorter coherence time is offset by slower reexcitation and stronger antibunching leading to similar peak visibilities compared to pairs of XX photons. The maximum measured visibilities of 0.57 ± 0.04 and 0.52 ± 0.03 indicate that the majority of copolarized XX or X photons interfere when coincidentally detected, and that the postselected XX and X photon components of subsequently emitted entangled photon pairs are indistinguishable.

High entanglement fidelity and high two-photon-interference visibility are required for quantum logic applications. For dc excitation, individual emission cycles cannot be isolated in time, thus entanglement and indistinguishability cannot be measured over a single wave packet. Instead, the figure of merits are the temporally postselected peak fidelity and visibility values, which require the detector response time to be faster than the time scales for evolution of the entangled state, or decoherence of interference, respectively. For this quantum dot, the shortest of these time scales is the coherence time, as the small FSS ensures a relatively slow evolution of the entangled state with period ~2.1 ns. To estimate the limitations of our interference measurements due to finite detector response time, two-photon-interference measurements were calculated based on independent measurements of τ_c, the temporal jitter of the detectors, and $g^{(2)}$, using models described elsewhere [22]. We note that correlations measured using a Hanbury Brown–Twiss intensity interferometer, are consistent with $g_{\mathrm{HBT}}^{(2)}(0) = 0$ convoluted with detector response [26]. As above, this indicates an improvement in background light rejection compared to our previous dc entanglement experiments [15]. The results of these calculations are presented in Figs. 2(e) and 2(f) as solid lines, which show excellent agreement without any free fitting parameters. Recalculation removing the effect of detector jitter is also shown as dashed lines, which illustrates that interference visibility of postselected photons emitted by our device

could potentially be close to 100%, due to negligible background light contributions.

Applications commonly require pulsed photon sources, which we explore by applying a sinusoidal ac voltage together with a dc bias. The operating frequency of 476 MHz is matched to the 2.1 ns interferometer delay, and is almost a factor of 6 higher than previously reported operating frequencies of optically or electrically excited quantum dot entangled light sources [12,15,27–30].

The XX coherence time is strongly dependent upon the ac voltage, falling from 219 to 70 ps as the amplitude is increased from 0.5 to 1.7 V [Fig. 3(a)]. The origin of the apparent decoherence is clear from inspection of the time-integrated spectrum, shown in Fig. 3(b), which shows an increase in the linewidth of the XX and X emission lines. We attribute the broadening to a time-dependent Stark shift of the emission line driven by the ac voltage [24], which is at a frequency comparable to the radiative decay rate. For the measurements below, we therefore select an ac amplitude of 0.5 V to maximize the observed coherence time. Time-resolved electroluminescence measured for the XX emission line is shown in Fig. 3(c), which demonstrates a strongly pulsed character. This can occur despite the sinusoidal driving field due to the superlinear response of the XX emission intensity with applied voltage.

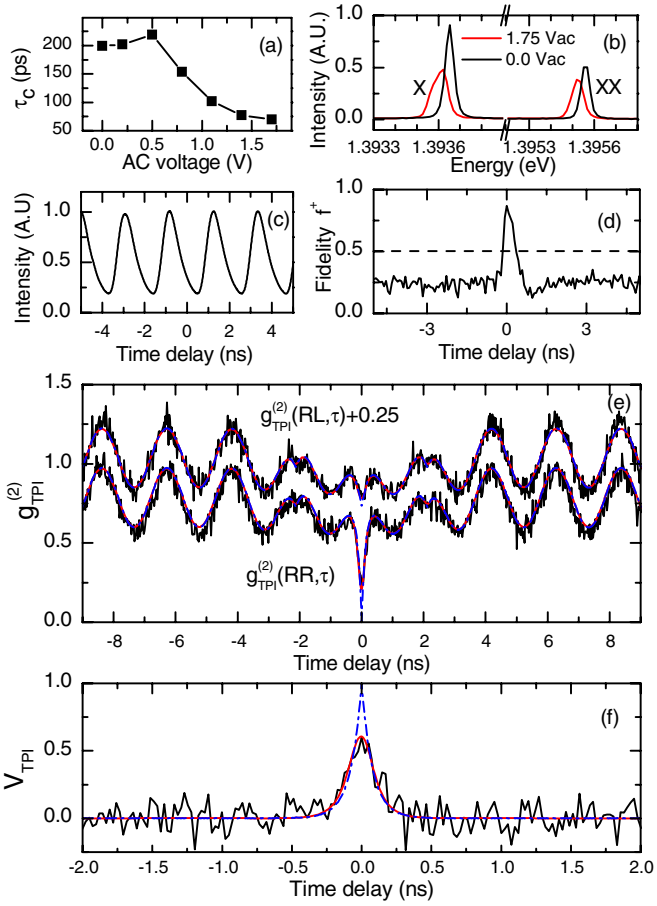

FIG. 3 (color online). Properties of ELED emission in ac mode. (a) Single XX photon coherence time as a function of ac amplitude. (b) Spectrum of emission from ELED under dc and strong ac excitation as indicated. (c) Time-resolved electroluminescence of XX emission under optimum ac excitation. (d) Fidelity f^+ of the emission to the entangled Bell state $|\Psi^+\rangle$. The classical limit of 0.5 is represented by a dashed line. (e) Second-order correlation of pairs of XX photons exiting the two-photon interferometer. The crosspolarized correlation $g^{(2)}_{\mathrm{TPI}}(\mathrm{RL},\tau)$ is vertically displaced by 0.25 so it may be distinguished from the copolarized correlation $g^{(2)}_{\mathrm{TPI}}(RR,\tau)$. (f) Visibility of XX TPI. Solid and dashed curves in (e) and (f) are simulated behavior for actual and ideal detector performance, respectively.

The entanglement fidelity and XX TPI correlations were measured in the same way as for dc excitation, and are shown in Figs. 3(d) and 3(e) respectively. The emission is entangled, with peak fidelity of 0.87 ± 0.04. The TPI correlations consist of a series of peaks spaced by multiples of the repetition period of 2.1 ns, due to the modulated nature of the emission. Correlation peaks centered at ± 4.2 ns or greater are not affected by the quantum nature of the source or TPI, and while not fully resolved due to jitter caused by the radiative lifetime of XX, are approximately double the intensity at their maxima than minima. In addition, the peaks at zero, and ± 2.1 ns are reduced further, due to the non-Poissonian nature of the quantum dot light source, as described above. Finally, the dip for the copolarized correlation is significantly deeper than measured in the crosspolarized correlation due to TPI. The TPI visibility is plotted in Fig. 3(f), which reveals a maximum visibility of 0.60 ± 0.05.

We calculate the expected two-photon-interference correlations using the model described above, approximating correlations for large delays as a sinusoid with period 2.1 ns. The results of calculations convoluted with the detector response are shown in Figs. 3(e) and 3(f) as solid lines and show a very good fit to the experimental data.

Finally, we note that for indistinguishable entangled photon pairs, detection of oppositely polarized photons in each output of a two-photon-interferometer, such as the above measurements of $g^{(2)}_{\mathrm{TPI}}(\mathrm{RL},\tau)$, performs an entanglement-swapping operation creating entanglement between the remaining photons of subsequent cycles. The fidelity of an entangled photon pair created via entanglement-swapping f^S is formulated by approximating the source entangled photons as a Bell state mixed with uncorrelated light, consistent with experiments, which leads to the following equation:

$$f^S = V\left((f^+)^2 + \frac{1}{3}(1-f^+)^2\right) + \frac{1-V}{4}.$$

Despite the imperfect observed entanglement fidelity of the initial photon pairs, and limited two-photon-interference visibility, we estimate that entangled photon pairs may be created this way with fidelity of 0.56 ± 0.05. In contrast,

for distinguishable input states or uncorrelated source photons, the above equation predicts a fidelity of 0.25, which corresponds to a fully mixed photon pair state. Thus the potential to perform entanglement swapping is a useful assessment of entanglement and indistinguishability of photon pairs.

While the above results focus on two-photon interference measured in the circular polarization basis, other measurement bases yield similar results. When measuring TPI in dc mode, the visibility in the circular, rectilinear, or diagonal bases has an average value of 0.52 and a standard deviation of 0.03. In contrast, entanglement measurements show slightly different polarization correlations in rectilinear, diagonal, and circular bases due to fine-structure splitting fixed in the rectilinear basis, and fluctuating in the circular basis due to nuclear spin interactions [31]. Our calculations show that fine-structure effects would have negligible influence in two-photon-interference experiments, supporting our observations.

In conclusion, we have presented entanglement fidelity and two-photon-interference visibility measurements that show photons originating from a semiconductor quantum dot are entangled with a simultaneously emitted photon, and indistinguishable from the next. The two-photon-interference measured here may be increased by using smaller, faster devices in pulsed mode to avoid reexcitation, with spontaneous emission rates enhanced by optical cavities to reduce the importance of detection time resolution. Such devices could lead to the generation, control, and interactions between large numbers of entangled photons required for practical quantum computing.

We thank A. Chan for useful input. We acknowledge partial support for this work from the Engineering and Physical Sciences Research Council, and the EU through the FP7 FET Q-ESSENCE Integrated Project and the Spin-Optronics ITN.

[1] E. Knill, R. Laflamme, and G. J. Milburn, Nature (London) **409**, 46 (2001).
[2] D. Bouwmeester, J.-W. Pan, M. Daniell, H. Weinfurter, and A. Zeilinger, Phys. Rev. Lett. **82**, 1345 (1999).
[3] C.-Y. Lu, X.-Q. Zhou, O. Guhne, W.-B. Gao, J. Zhang, Z.-S. Yuan, A. Goebel, T. Yang, and J.-W. Pan., Nature Phys. **3**, 91 (2007).
[4] C. K. Hong, Z. Y. Ou, and L. Mandel, Phys. Rev. Lett. **59**, 2044 (1987).
[5] T. B. Pittman, M. J. Fitch, B. C Jacobs, and J. D. Franson, Phys. Rev. A **68**, 032316 (2003).
[6] J. L. O-Brien, G. J. Pryde, A. G. White, T. C. Ralph, and D. Branning, Nature (London) **426**, 264 (2003).
[7] S. Gasparoni, J.-W. Pan, P. Walther, T. Rudolph, and A. Zeilinger, Phys. Rev. Lett. **93**, 020504 (2004).
[8] C.-Y. Lu, D. E. Browne, T. Yang, and J.-W. Pan, Phys. Rev. Lett. **99**, 250504 (2007).
[9] B. P. Lanyon, T. J. Weinhold, N. K. Langford, M. Barbieri, D. F. V. James, A. Gilchrist, and A. G. White, Phys. Rev. Lett. **99**, 250505 (2007).
[10] V. Scarani, H. de Riedmatten, I. Marcikic, H. Zbinden, and N. Gisin, Eur. Phys. J. D **32**, 129 (2004).
[11] P. Michler, A. Kiraz, C. Becher, W. V. Schoenfeld, P. M. Petroff, Lidong Zhang, E. Hu, and A. Imamoglu, Science **290**, 2282 (2000).
[12] R. M. Stevenson, R. J. Young, P. Atkinson, K. Cooper, D. A. Ritchie, and A. J. Shields, Nature (London) **439**, 179 (2006).
[13] C. Santori, D. Fattal, J. Vuckovic, G. S. Solomon, and Y. Yamamoto, Nature (London) **419**, 594 (2002).
[14] A. J. Bennett, M. A. Pooley, R. M. Stevenson, M. B. Ward, R. B. Patel, A. B. de la Giroday, N. Sköld, I. Farrer, C. A. Nicoll, D. A. Ritchie, and A. J. Shields, Nature Phys. **6**, 947 (2010).
[15] C. L. Salter, R. M. Stevenson, I. Farrer, C. A. Nicoll, D. A. Ritchie, and A. J. Shields, Nature (London) **465**, 594 (2010).
[16] J.-W. Pan, D. Bouwmeester, H. Weinfurter, and A. Zeilinger, Phys. Rev. Lett. **80**, 3891 (1998).
[17] H.-J. Briegel, W. Dür, J. I. Cirac, and P. Zoller, Phys. Rev. Lett. **81**, 5932 (1998).
[18] J.-W. Pan, C. Simon, C. Brukner, and A. Zeilinger, Nature (London) **410**, 1067 (2001).
[19] Oliver Benson, Charles Santori, Matthew Pelton, and Yoshihisa Yamamoto, Phys. Rev. Lett. **84**, 2513 (2000).
[20] R. J. Young, R. M. Stevenson, A. J. Shields, P. Atkinson, K. Cooper, D. A. Ritchie, K. M. Groom, A. I. Tartakovskii, and M. S. Skolnick, Phys. Rev. B **72**, 113305 (2005).
[21] R. B. Patel, A. J. Bennett, K. Cooper, P. Atkinson, C. A. Nicoll, D. A. Ritchie, and A. J. Shields, Phys. Rev. Lett. **100**, 207405 (2008).
[22] R. B. Patel, A. J. Bennett, K. Cooper, P. Atkinson, C. A. Nicoll, D. A. Ritchie, and A. J. Shields, Nanotechnology **21**, 274011 (2010).
[23] A. J. Hudson, R. M. Stevenson, A. J. Bennett, R. J. Young, C. A. Nicoll, P. Atkinson, K. Cooper, D. A. Ritchie, and A. J. Shields, Phys. Rev. Lett. **99**, 266802 (2007).
[24] A. J. Bennett, R. B. Patel, A. J. Shields, K. Cooper, P. Atkinson, C. A. Nicoll, and D. A. Ritchie, Appl. Phys. Lett. **92**, 193503 (2008).
[25] S. Ates, S. M. Ulrich, S. Reitzenstein, A. Löffler, A. Forchel, and P. Michler, Phys. Rev. Lett. **103**, 167402 (2009).
[26] See Supplemental Material at http://link.aps.org/supplemental/10.1103/PhysRevLett.108.040503 for additional description of source properties, and measurement techniques.
[27] R. Hafenbrak, S. M. Ulrich, P. Michler, L. Wang, A. Rastelli, and O. G. Schmidt, New J. Phys. **9**, 315 (2007).
[28] A. Muller, W. Fang, J. Lawall, and G. S. Solomon, Phys. Rev. Lett. **103**, 217402 (2009).
[29] A. Mohan, M. Felici, P. Gallo, B. Dwir, A. Rudra, J. Faist, and E. Kapon, Nature Photon. **4**, 302 (2010).
[30] A. Dousse, J. Suffczynski, A. Beveratos, O. Krebs, A. Lemaître, I. Sagnes, J. Bloch, P. Voisin, and P. Senellart, Nature (London) **466**, 217 (2010).
[31] R. M. Stevenson, C. L. Salter, A. Boyer de la Giroday, I. Farrer, C. A. Nicoll, D. A. Ritchie, and A. J. Shields, arXiv:1103.2969v1.